

# Complementarity and quantum erasure with entangled-photon states

Tedros Tsegaye and Gunnar Björk\*

*Department of Electronics, Royal Institute of Technology (KTH), Electrum 229, 164 40 Kista, Sweden*

Mete Atatüre,<sup>2</sup> Alexander V. Sergienko,<sup>1</sup> Bahaa E. A. Saleh,<sup>1</sup> and Malvin C. Teich<sup>1,2</sup>

<sup>1</sup>*Quantum Imaging Laboratory, Department of Electrical and Computer Engineering*

<sup>2</sup>*Quantum Imaging Laboratory, Department of Physics, Boston University, 8 Saint Mary's Street, Boston, Massachusetts 02215*

(Received 22 October 1999; published 18 August 2000)

A quantum-erasure experiment was performed on superposition states of two photons in either of two spatiotemporal modes. Symmetrical tapping of energy from the two-mode state creates a four-mode entangled state. A direct measurement of one photon in two of the modes reveals the path of the second one, thereby eliminating the possibility of observing interference between the two remaining modes. It is shown that a unitary rotation of one of the two-mode states erases the path information; as a consequence, the visibility of the other two-mode state can be resurrected.

PACS number(s): 03.65.Bz, 42.50.Dv, 42.65.Ky

## I. INTRODUCTION

Complementarity, the presence in a physical system of two properties that cannot simultaneously be known precisely, has attracted great interest since the early days of quantum mechanics. Wave-particle duality, which represents the complementary nature of the wavelike and particlelike behaviors of a quantum system, is perhaps the example that has garnered the greatest share of attention. The wavelike behavior is manifested in interference experiments. However, when a *welcher-weg* (which-path) measurement is carried out on an interfering system, the system becomes entangled with the measuring apparatus, so that the paths of the system become distinguishable, and the fringe visibility vanishes. In recent years several quantitative expressions of this specific duality have been discussed [1–10] and experimentally confirmed [11–18]. If the which-path detector is also a quantum system, the distinguishability could be erased while the interference is restored. Experiments along this line, first proposed by Scully and Drühl [19], are called quantum-erasure experiments, and have been discussed extensively in connection with complementarity [4,10,13,14,16–18,20,21].

One aspect of complementarity that has been particularly debated is the particular physical mechanism that enforces it [6,7,22–24], and further to what extent complementarity, expressed for example by the inequality derived by Englert [9] [Eq. (4) below], is a statement of complementarity independent of the Heisenberg [25] or Schrödinger-Robertson uncertainty principles [7,9,21,22,26]. The two issues are interconnected, as it has been argued that the which-path measurement is always connected by a random momentum kick that destroys the possibility of obtaining interference fringes [7,22]. This issue has been shown to be rather subtle as quantum mechanics allows the possibility of different definitions as to what constitutes a random kick [24]. It has recently been argued, in fact, that many which-path and quantum-erasure measurements involve measurement of nei-

ther position nor momentum [21,27,28]. In particular, Luis and Sánchez-Soto [27] showed that in experiments in which the path determination can be described within a two-dimensional Hilbert space, the “kicked” observable is phase difference rather than momentum. The experiments reported in Refs. [11–15], and the experiment reported below, fall within this category whereas, for example, the experiment originally proposed in Ref. [19] and the experiments reported in Refs. [16,17], do not.

In this paper we report an even more dramatic experiment in which a large and deliberate change is applied to the internal state of the object. Nevertheless the complementary character of the wavelike and particlelike behavior is maintained.

## II. A QUANTUM-ERASURE EXPERIMENT BASED ON ENTANGLED-PHOTON STATES

Central to the discussion about what physical mechanism enforces complementarity has been the extent of momentum transfer imparted by a which-path measurement. In this paper we present a scheme where the state before the which-path measurement is a superposition state with two photons in either of the paths, or more correctly, in either of two spatiotemporal modes. By symmetrically tapping energy from both of the modes, one of the two photons can be used to gain path information about the remaining photon (Fig. 1). On an identically prepared ensemble we measure the visibility of interference fringes (Fig. 2).

By postselection, using a coincidence technique, only states in which one photon is reflected and one photon is transmitted by either of the beam splitters ( $BS_2$  or  $BS_3$ ), are chosen. In the following discussion the reflected photon will be denoted the “meter photon” and the transmitted photon as the “object photon.” This choice is arbitrary, as seen from the symmetry between the transmitted modes and the reflected modes. When the meter is set to give which-path information, i.e., when beam splitter  $BS_4$  has zero or unity reflectance, the fringe visibility of the object vanishes. A unitary transformation by the meter state “quantum erases”

\*Electronic address: gunnarb@ele.kth.se

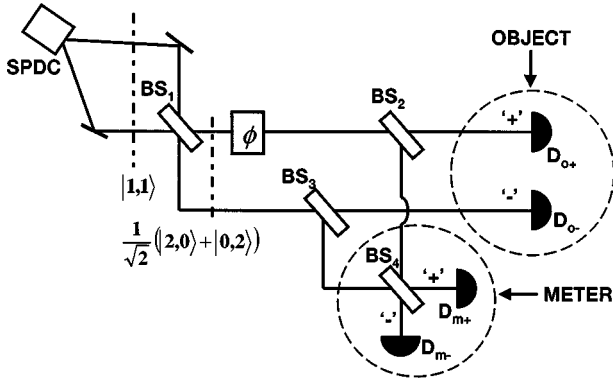


FIG. 1. Distinguishability measurement. The photon pair produced by spontaneous parametric down-conversion (SPDC) impinges on beam splitter  $BS_1$ . Beam splitters  $BS_2$  and  $BS_3$  are used to tap one photon. The modes of the reflected photon (the “meter photon”) are mixed by beam splitter  $BS_4$ . The beam splitters  $BS_1$ ,  $BS_2$ , and  $BS_3$  have 50%-50% reflectance and transmittance whereas the reflectance of  $BS_4$  may vary. The single photon detectors  $D_{o+}$  and  $D_{o-}$  monitor whether the “object photon” takes the “+” or “-” path. Similarly the detectors  $D_{m+}$  and  $D_{m-}$  tell which path, “+” or “-,” is taken by the “meter photon.”

the which-path information while providing conditioned fringe visibility, and hence information about the phase difference is revealed. In the depicted setup this unitary transformation is accomplished by choosing the reflectivity of  $BS_4$  to be 50%. In this case there is no way of knowing from which of the two ports of  $BS_1$  the photon originated.

Our path determination measurement does not preserve the photon number of the object modes, and therefore the momentum of the object will change as a consequence of the measurement. In the present experiment the change is substantial: half of the momentum of the initial state (the two-photon superposition state) is lost to the meter mode. This large, and deliberate, object disturbance in comparison with previous quantum-erasure experiments is the principal interest of our scheme. We discuss the implications below.

Given the outcome of the meter measurement the likelihood  $L$  of guessing the right path for the object is [8,9]

$$L = \text{Max}(w_{++}, w_{+-}) + \text{Max}(w_{-+}, w_{--}), \quad (1)$$

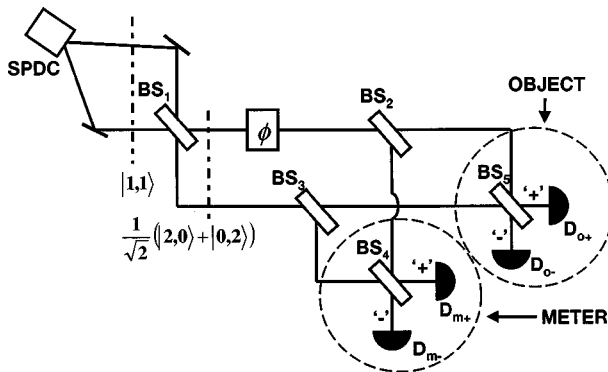


FIG. 2. Visibility measurement. The setup is identical to that shown in Fig. 1 except that the modes of the transmitted photon (the “object photon”) are mixed by the 50%-50% beam splitter  $BS_5$ .

where  $w_{mo}$  denotes the probability that the meter photon is detected by detector  $m$  and that the object photon is detected by detector  $o$ , and where  $m$  and  $o$  are either “+” or “-” (see Fig. 1). A normalized quantitative measure of the which-path information is given by the distinguishability  $D$  defined by [9]

$$D = 2L - 1 = |w_{++} - w_{+-}| + |w_{-+} - w_{--}|. \quad (2)$$

The setup for measuring the visibility of quantum interference is shown in Fig. 2. The visibility is given by

$$V = \frac{\text{Max}_\phi(w_{++}) - \text{Min}_\phi(w_{++})}{\text{Max}_\phi(w_{++}) + \text{Min}_\phi(w_{++})}, \quad (3)$$

where, e.g.,  $\text{Max}_\phi(w_{++})$  denotes the maximum value of the probability  $w_{++}$  as the phase shift  $\phi$  is increased from zero to  $\pi$ . Due to the symmetry of the setup, the value of this expression is identical under the transformation  $+ \rightarrow -$  for either or both indices.

The which-path information given by the distinguishability  $D$ , and the phase information given by the visibility  $V$ , is limited by the inequality [8,9]

$$V^2 + D^2 \leq 1. \quad (4)$$

Consider an ideal experiment such as that depicted in Figs. 1 and 2. If  $D = 1$ , the paths of the object are completely distinguishable and the interference is lost, i.e.,  $V = 0$ . If, on the other hand,  $D = 0$ , the outcome from the meter measurement does not reveal any information about the path of the object, but interference is fully restored, i.e.,  $V = 1$ .

When a pair of down-converted photons with the same energy and polarization interacts with a 50%-50% beam splitter, a Schrödinger-cat-like state is produced:

$$\Psi^{(2)} = |1,1\rangle \Rightarrow \Psi^{(2)} = \frac{1}{\sqrt{2}}(|2,0\rangle + |0,2\rangle); \quad (5)$$

the notation  $|a,b\rangle$  indicates that  $a$  is the photon number in the “+” path and  $b$  is the photon number in the “-” path. A measurement of the photon numbers in the outgoing ports of the beam splitter reveals that the photons are grouped. When the state propagates through a phase shifter  $\phi$ , a total relative phase of  $2\phi$  is accumulated. This is a manifestation of the de Broglie wavelength of the two-photon state, as pointed out in Refs. [29–31]:

$$\Psi^{(2)} = \frac{1}{\sqrt{2}}(e^{2i\phi}|2,0\rangle + |0,2\rangle). \quad (6)$$

In the original Hong-Ou-Mandel experiment [29], the interference effects associated with the state in Eq. (6) is shown. In our experiment we tap out one photon from the state in Eq. (6) with beam splitters  $BS_2$  and  $BS_3$ . The state then is transformed to a four-mode entangled state

$$\Psi^{(2)} = \frac{1}{2} \left[ \left( i|1,0,1,0\rangle + \frac{|2,0,0,0\rangle}{\sqrt{2}} - \frac{|0,0,2,0\rangle}{\sqrt{2}} \right) e^{2i\phi} + \left( i|0,1,0,1\rangle + \frac{|0,2,0,0\rangle}{\sqrt{2}} - \frac{|0,0,0,2\rangle}{\sqrt{2}} \right) \right], \quad (7)$$

where the notation  $|a,b,c,d\rangle$  indicates the following:  $a$  is the photon number in the “+” path of the object,  $b$  is photon number in the “-” path of the object,  $c$  is the photon number in the “+” path of the meter, and  $d$  is the photon number in the “-” path of the meter. We look for the distinguishability between the “+” and “-” modes of the object and the visibility when the “+” and “-” modes of the object interfere, on condition that one photon is detected by either the “+” or “-” meter detector. In the experiment, we record the coincidence counts only from the events when one of the object detectors fires and one of the meter detectors fires; thus by post-selection the state in Eq. (7) reduces to

$$\Psi^{(2)} = \frac{1}{\sqrt{2}} (|1,0,1,0\rangle e^{2i\phi} + |0,1,0,1\rangle). \quad (8)$$

After the meter photon passes through  $BS_4$ , with reflectance  $R_4 = \sin^2(\theta)$ , the post-selected state is

$$\Psi^{(2)} = \frac{1}{\sqrt{2}} [ |1,0\rangle (\cos(\theta)|1,0\rangle + i \sin(\theta)|0,1\rangle) e^{2i\phi} + |0,1\rangle (\cos(\theta)|0,1\rangle + i \sin(\theta)|1,0\rangle) ]. \quad (9)$$

By varying the reflectance  $R_4$ , we can observe that the object, conditioned of a sharp measurement of the meter state, will demonstrate a transition from particlelike to wavelike behavior.

The distinguishability computed using Eq. (2) will then be

$$D = |\cos^2(\theta) - \sin^2(\theta)| = |\cos(2\theta)|, \quad (10)$$

whereas the visibility, given by Eq. (3), is

$$V = 2 |\cos(\theta) \sin(\theta)| = |\sin(2\theta)|. \quad (11)$$

If the reflectance  $R_4 = 0$ , or  $R_4 = 1$ , the meter reveals full information on which of the paths in Fig. 1 the object photon takes. For this case there is no interference (Fig. 2). If  $R_4 = 1/2$ , the which-path information is fully erased but the visibility is restored. When the object path goes through a 50%-50% beam splitter, as in Fig. 2, full contrast interference fringes appear for the interference data, which is sorted in two sets according to which of the detectors  $D_{m+}$  or  $D_{m-}$  fires. It is clear from Eq. (9) that one of the interference data sets has a maximum where the other set has its minimum; otherwise they are identical for any value of  $\theta$ . Therefore, if the outcome of the measurement of the meter state is ignored (i.e., the two sets of data are mixed), no interference can be seen. The measurement constitutes a *quantum eraser* since

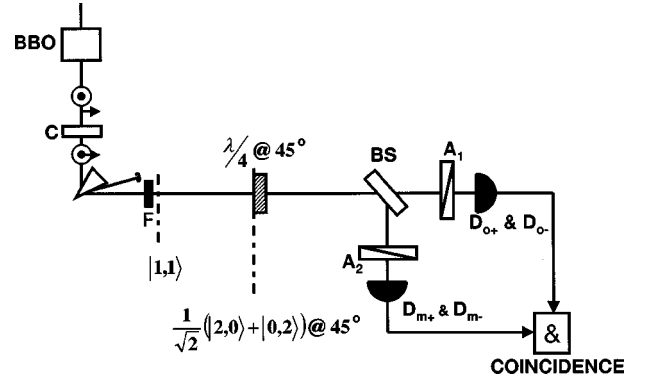


FIG. 3. A photon pair produced in BBO via type-II spontaneous parametric down-conversion impinges on a compensator plate  $C$  (used to make the two photons overlap in time) and thence on a filter  $F$  (used to narrow the spectral width of the pair). In a basis rotated by  $45^\circ$ , the photon pair is described by a Schrödinger-cat-like state. A quarter-wave plate inserted with the fast axis at  $45^\circ$  with respect to the vertical axis gives rise to a phase shift of  $\pi/2$ . By rotating analyzer  $A_1$  to  $45^\circ$  or  $135^\circ$  a distinguishability measurement similar to that shown in Fig. 1 is performed. When  $A_1$  is set to  $0^\circ$  or  $90^\circ$ , the setup corresponds to that shown in Fig. 2. The analyzer  $A_2$  is set at different angles  $\xi = 45^\circ - \theta$  with respect to the vertical axis; this corresponds to a variable transmittance  $T = \cos^2 \theta$  of beam splitter  $BS_4$  in Figs. 1 and 2.

the distinguishability is erased and the interference is restored, both contingent on the use of the meter-state measurement.

### III. EXPERIMENTAL ARRANGEMENT AND RESULTS

Spontaneous parametric down-conversion (SPDC) is a method that has often been used to produce photon pairs. In this process a pump photon is converted into a pair of photons with lower energy. SPDC is possible in nonlinear, birefringent materials via the conservation of energy  $\omega_p = \omega_s + \omega_i$  and momentum  $\mathbf{k}_p = \mathbf{k}_s + \mathbf{k}_i$ , where the subscripts refer to the pump ( $p$ ) and the down-converted photons, usually denoted signal ( $s$ ) and idler ( $i$ ). There are two types of SPDC; in type-I SPDC the signal and idler have the same polarization, whereas in type-II SPDC they are orthogonally polarized. To minimize the influence of mechanical vibrations and drift we used an interferometer in which the photons are in the same spatio-temporal mode but in orthogonal polarization modes (vertical and horizontal). The setup is topologically equivalent to the spatial interferometer shown in Figs. 1 and 2, and is shown in Fig. 3. Similar setups have been used for other measurements of fringe visibility [32]. An adjustable birefringent delay line is used to compensate for the dispersion from the birefringent SPDC crystal. The state after the nonlinear crystal and the compensator, in the horizontal and vertical ( $0^\circ$  and  $90^\circ$ ) bases, is

$$\Psi^{(2)} = |1,1\rangle = a_0^\dagger a_{90}^\dagger |0\rangle, \quad (12)$$

where  $a_\eta^\dagger$  is the creation operator of the polarization mode at  $\eta^\circ$  with respect to the vertical axis. The relative phase shift is applied in a rotated base, which has a  $45^\circ$  angle with

respect to the vertical and horizontal axes. In this coordinate system the photons are in the state given in Eq. (5)

$$\Psi^{(2)} = \frac{(a_{45}^\dagger - a_{135}^\dagger)|0\rangle}{\sqrt{2}} = \frac{1}{\sqrt{2}}(|2,0\rangle - |0,2\rangle). \quad (13)$$

With the notation  $|a,b\rangle$  in the current case,  $a$  denotes the photon number of the polarization mode at  $45^\circ$  with respect to the vertical axis, and  $b$  denotes the photon number of the polarization mode at  $135^\circ$  with respect to the vertical axis. The functions of the beam splitters  $BS_1$  and  $BS_2$ , depicted in Figs. 1 and 2, are physically combined into one polarization-independent beam splitter BS. There are two analyzers, one for each arm. For the visibility measurement the analyzer  $A_1$  of the transmitted beam is oriented either so that vertical ( $0^\circ$ ) or horizontal ( $90^\circ$ ) light is transmitted, corresponding to the “+” path or “-” path in Fig. 2. For the distinguishability measurement the analyzer  $A_1$  is oriented at either  $45^\circ$  or  $135^\circ$ , corresponding to the “+” path or “-” path in Fig. 1.

After passing through the phase shift and the beam splitter the state of interest that will be post-selected is

$$\begin{aligned} \Psi^{(2)} = & \cos(\phi)(|0,1,1,0\rangle - |1,0,0,1\rangle) \\ & + i \sin(\phi)(|1,0,1,0\rangle - |0,1,0,1\rangle), \end{aligned} \quad (14)$$

expressed in the horizontal-polarized-object, and vertical-polarized-object, horizontal-polarized-meter, and vertical-polarized-meter bases. In the  $45^\circ$ - and  $135^\circ$ - polarized-object and  $45^\circ$ - and  $135^\circ$ - polarized-meter bases, the state can be written as

$$\Psi^{(2)} = \frac{1}{\sqrt{2}}(|1,0,0,1\rangle e^{i\phi} - |0,1,1,0\rangle e^{-i\phi}). \quad (15)$$

For the reflected arm the analyzer  $A_2$  is set at different angles  $\xi = 45 - \theta$  from the vertical axis. The analyzer  $A_2$ , together with the detector, corresponds to the “+” path of the meter preceded by a beam splitter with transmittance  $\cos^2 \theta$  (or the “-” path of the meter preceded by a beam splitter with transmittance  $\sin^2 \theta$ ). The state of the object, depending on the outcome of the meter, is

$$\Psi^{(2)} = i \sin(\theta)|1,0\rangle e^{i\phi} - \cos(\theta)|0,1\rangle e^{-i\phi}. \quad (16)$$

The distinguishability between the object states  $|1,0\rangle$  and  $|0,1\rangle$  (in the  $45^\circ$  and  $135^\circ$  bases) is given by Eq. (10).

Projected to the horizontal and vertical basis (corresponding to passing through the 50%-50% beam splitter  $BS_5$  in the spatial interferometer in Fig. 3) the state of the object is

$$\begin{aligned} \Psi^{(2)} = & \frac{i|1,0\rangle}{\sqrt{2}}(\sin(\theta)e^{i\phi} - \cos(\theta)e^{-i\phi}) \\ & - \frac{|1,0\rangle}{\sqrt{2}}(\sin(\theta)e^{i\phi} + \cos(\theta)e^{-i\phi}), \end{aligned} \quad (17)$$

and the visibility is the same as Eq. (11).

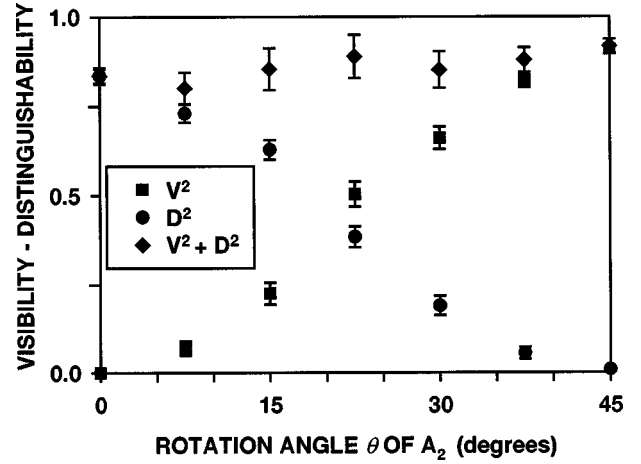


FIG. 4. Experimentally measured values of the squared visibility  $V^2$  (squares), squared distinguishability  $D^2$  (circles), and their sum  $V^2 + D^2$  (triangles) are displayed as a function of the angle  $\theta$  of analyzer  $A_2$  shown in Fig. 3, corresponding to a transmittance  $T = \cos^2 \theta$  for beam splitter  $BS_4$  in Figs. 1 and 2.

Our light source is a single-mode argon-ion laser with a wavelength of 351.1 nm. The SPDC crystal is  $\beta$ -BaB<sub>2</sub>O<sub>4</sub> (BBO) with a length 0.5 mm. The crystal is aligned so that collinear orthogonally polarized photon pairs with equal energy are produced. The pump is separated from the photon pairs by a dispersion prism. Pinholes and one interference filter, with a bandwidth of 10 nm and centered at 702.2 nm, further select photon pairs that have the same energy and that travel in the same spatiotemporal mode. Due to the linear dispersion of the crystal the horizontally and vertically polarized photons are separated in time. A birefringent crystal-line quartz delay line is used to compensate for the linear dispersion, which makes the two orthogonally polarized photons overlap in time [33]. The detectors are actively quenched single-photon-counting modules (EG&G SPCM).

The experimental data presented are just as collected (raw data) without any background subtraction. In Fig. 4 the squared visibility  $V^2$  and the squared distinguishability  $D^2$  are plotted as a function of the angle  $\theta$  of analyzer  $A_2$ . When the analyzer  $A_1$  is set at  $0^\circ$  or  $90^\circ$ , the measurement exhibits interference effects and the visibility goes from  $0.04 \pm 0.04$  for  $\theta = 0^\circ$  to  $0.95 \pm 0.04$  for  $\theta = 45^\circ$  (squares in Fig. 4). The distinguishability goes from  $0.10 \pm 0.04$  for  $\theta = 45^\circ$  to  $0.91 \pm 0.04$  for  $\theta = 0^\circ$  (circles in Fig. 4). We have also plotted  $V^2 + D^2$  (triangles in Fig. 4). This shows the complementarity between particlelike (which-path information) and wave-like (interference) behaviors. When  $\theta$  goes from  $0^\circ$  to  $45^\circ$  the which-path information is (quantum) erased, and the interference is restored.

At first glance one would expect that the measured sum  $D^2 + V^2$  would be greatest when  $D$  was maximized, since the measurement of  $D$  essentially follows directly from energy conservation. The measurement of  $V$ , on the other hand, requires interference and hence careful mode matching to agree with theory. From Fig. 4 it is seen that we observe the opposite result, the sum  $D^2 + V^2$  is actually greatest when  $V$  is close to unity. The reason for this, we believe, is due to

imperfect dispersion cancellation between the vertically and horizontally polarized photon impinging on the  $\lambda/4$  plate. Consequently the two photons are slightly distinguishable and will not form the perfect entangled-photon state of Eq. (13). Instead the state is in a mixture between the desired entangled-photon state and a  $|1,1\rangle$  state (in the  $45^\circ$  and  $135^\circ$  bases). This latter state will lead to an unentangled object and meter state by the subsequent energy tapping by the beam splitter, and deteriorate the quality of the distinguishability measurement.

An important issue, which has not been discussed extensively in the context of quantum erasure, is the fact that the necessary entanglement between the object and the meter can be essentially of two types. Path identification necessarily involves a sharp measurement of the object. However, *what* is being measured to establish the path of the object differs from experiment to experiment. In the experiment described above it involves a photon-number measurement of the two object modes, the  $+$  mode and the  $-$  mode. It is then possible to classify the interaction Hamiltonian  $\hat{H}_i$  responsible for entangling the object and meter degrees of freedom into two classes, depending on whether  $\hat{H}_i$  commutes with the measurement observable(s) or not. In general it is desirable that it does commute, because this means that the *probability* of finding the object in a particular state does not change as a consequence of the meter entanglement interaction. (The combined object and meter *state*, on the other hand, must change, going from a factorizable form to a nonfactorizable form for an entangled state.) In Ref. [21] such a Hamiltonian, which commutes with the appropriate which-path observable, has been referred to as a quantum-nondemolition (QND)-type Hamiltonian since a perfect entanglement of this type, and subsequent sharp measurement of the meter mode, effectively constitutes a perfect QND measurement of the path. The interaction Hamiltonian in the experiment we have performed is of the other class. The entanglement is performed by splitting the state of Eq. (13) in a beam splitter. The interaction Hamiltonian  $\hat{H}_i = \pi(\hat{a}\hat{c}^\dagger + \hat{a}^\dagger\hat{c} + \hat{b}\hat{d}^\dagger + \hat{b}^\dagger\hat{d})/4$  [where the labeling follows that in Eq. (7)] is of the Jaynes-Cummings form, and does not commute with the which-path observables which are  $\hat{n}_a = \hat{a}^\dagger\hat{a}$  and  $\hat{n}_b = \hat{b}^\dagger\hat{b}$ . Therefore, as discussed in Ref. [10], the object changes its “internal” state; that is, the probability of finding the object in a certain state changes as a consequence of interaction between the object and the meter. In this more general case, a more extended analysis [10] of complementarity is required than that expressed by the quantitative expression in Eq. (4).

The principal additional complication with the noncommuting scheme is of a philosophical nature, and has to do with the definition of the word “object.” The easiest way of dealing with this difficulty is to define the object in terms of a pair of specific states, one representing the object being in the upper path and the other representing the object being in the lower path. In our experiment the pertinent object states would be  $|2,0\rangle$  and  $|0,2\rangle$ . However, this definition of an object has the complication that if the interaction between the object and meter changes the state of the object, the

object, by definition, ceases to exist. Hence the states  $|1,0\rangle$  and  $|0,1\rangle$  would have no significance, although we know that with the particular interaction Hamiltonian used in our experiment, e.g., the preinteraction state  $|2,0\rangle$ , is uniquely associated with the postinteraction state  $|1,0\rangle$  and that both therefore can be associated with the same object path. The definition of the object in terms of a pair of states is also at odds with our casual understanding of the term. In our everyday use of the word we usually disregard the particular state of the object. Thus, for example, a Rb atom is a Rb atom whether it is in an excited state or in its ground state. Hence, in a similar experiment to ours, where an excited Rb atom is prepared in a superposition of two spatiotemporal modes, and a photon is emitted into a set of meter modes in such a way as to enable path identification, it would be quite natural to speak about the post-interaction, ground-state Rb atom as the object but in a different “internal” state. However, using photon-number states as object states it is less natural, but still reasonable, to view the states  $|n,0\rangle$  and  $|n-1,0\rangle$  as two different “internal” states of the same object. Our experiment highlights this contradiction between the two ways of defining the object.

We have avoided most of the complications (both experimental and semantic) associated with a multiple “internal” state object by excluding all but two orthogonal object states by post-selection. As have been shown, both path determination and subsequent quantum erasure works nearly perfectly (the discrepancy stems from experimental imperfections) although half the energy and the linear momentum of the biphotons of the desired entangled-photon state [Eq. (13)] are taken away by the object-meter-state interaction. Still, the two ways of analyzing the experiment, in terms of information gained [quantitatively expressed by Eq. (4)], or in terms of phase-difference kicks, predict correctly that total quantum erasure is possible. This is not so surprising since it has long been known that information must always be represented by physical systems [34] and, conversely, that information theory can be used to describe pure, closed quantum systems. If one prefers to interpret this experiment from an information science point of view or a physics point of view it is therefore largely a matter of personal preference.

#### IV. CONCLUSION

To conclude, we have performed a complementarity experiment with a different kind of object. The initial object in our case, the entangled-photon state of Eq. (13) is in a superposition state of two quanta in either mode while previous quantum-mechanical experiments have all used “single-particle” objects (it is also possible to perform erasure experiments that can be explained in terms of classical physics [35]). Furthermore, in our experiment the interaction Hamiltonian between meter and object is not of the QND type, and as a consequence the state of the object changes radically as a consequence of the object-meter interaction. Yet, as the composite

postselected system is a nearly maximally entangled pure state, quantum erasure still works well. As well as examining the particlelike and wavelike behaviors, we also examine the intermediate cases in which the which-path information of the particlelike behavior gradually is erased and is replaced by visibility and wavelike behavior.

## ACKNOWLEDGMENTS

This work was funded by the Swedish Foundation for Strategic Research, the John och Karin Engbloms Stipendiefond, the Boston University Photonics Center, and the U.S. National Science Foundation.

- 
- [1] W. K. Wootters and W. H. Zurek, *Phys. Rev. D* **19**, 473 (1979).
- [2] D. M. Greenberger and A. Yasin, *Phys. Lett. A* **128**, 391 (1988).
- [3] L. Mandel, *Opt. Lett.* **16**, 1882 (1991).
- [4] M. O. Scully, B.-G. Englert, and H. Walther, *Nature (London)* **351**, 111 (1991).
- [5] M. G. Raymer and S. B. Yang, *J. Mod. Opt.* **39**, 1221 (1992).
- [6] R. Bhandari, *Phys. Rev. Lett.* **69**, 3720 (1992).
- [7] S. M. Tan and D. F. Walls, *Phys. Rev. A* **47**, 4663 (1993).
- [8] G. Jaeger, A. Shimony, and L. Vaidman, *Phys. Rev. A* **51**, 54 (1995).
- [9] B.-G. Englert, *Phys. Rev. Lett.* **77**, 2154 (1996).
- [10] G. Björk and A. Karlsson, *Phys. Rev. A* **58**, 3477 (1998).
- [11] Z. Y. Ou, L. J. Wang, X. Y. Zou, and L. Mandel, *Phys. Rev. A* **41**, 566 (1990); *Z. Y. Ou, Phys. Lett. A* **226**, 323 (1997).
- [12] X. Y. Zou, L. J. Wang, and L. Mandel, *Phys. Rev. Lett.* **67**, 318 (1991); A. G. Zajonc, L. J. Wang, X. Y. Zou, and L. Mandel, *Nature (London)* **353**, 507 (1991).
- [13] P. G. Kwiat, A. M. Steinberg, and R. Y. Chiao, *Phys. Rev. A* **45**, 7729 (1992).
- [14] T. J. Herzog, P. G. Kwiat, H. Weinfurter, and A. Zeilinger, *Phys. Rev. Lett.* **75**, 3034 (1995).
- [15] T. B. Pittman, D. V. Strekalov, A. Migdall, M. H. Rubin, A. V. Sergienko, and Y. H. Shih, *Phys. Rev. Lett.* **77**, 1917 (1996).
- [16] S. Dürr, T. Nonn, and G. Rempe, *Phys. Rev. Lett.* **81**, 5705 (1998).
- [17] Y.-H. Kim, R. Yu, S. P. Kulik, Y. H. Shih, and M. O. Scully, Los Alamos e-print, quant-ph/9903047.
- [18] P. D. D. Schwindt, P. G. Kwiat, and B.-G. Englert, e-print, quant-ph/9908072.
- [19] M. O. Scully and K. Drühl, *Phys. Rev. A* **25**, 2208 (1982).
- [20] P. G. Kwiat, A. M. Steinberg, and R. Y. Chiao, *Phys. Rev. A* **49**, 61 (1994).
- [21] G. Björk, J. Söderholm, A. Trifonov, T. Tsegaye, and A. Karlsson, *Phys. Rev. A* **60**, 1874 (1999).
- [22] P. Storey, S. Tan, M. Collett, and D. Walls, *Nature (London)* **367**, 626 (1994).
- [23] B.-G. Englert, M. O. Scully, and H. Walther, *Nature (London)* **375**, 367 (1995); E. P. Storey, S. M. Tan, M. J. Collett, and D. F. Walls, *ibid.* **375**, 368 (1995).
- [24] H. M. Wiseman and F. E. Harrison, *Nature (London)* **377**, 584 (1995); H. M. Wiseman, F. E. Harrison, M. J. Collett, S. M. Tan, D. F. Walls, and R. B. Killip, *Phys. Rev. A* **56**, 55 (1997).
- [25] W. Heisenberg, *Z. Phys.* **43**, 172 (1927).
- [26] E. Schrödinger, *Proc. Prussian Academy of Sciences Physics-Mathematics Sec.* , **XIX**, 296 (1930); H. P. Robertson, *Phys. Rev.* **35**, 667(A) (1930); **46**, 794 (1934).
- [27] A. Luis and L. L. Sánchez-Soto, *Phys. Rev. Lett.* **81**, 4031 (1998).
- [28] W. M. de Muynck, Los Alamos e-print, quant-ph/9901010.
- [29] C. K. Hong, Z. Y. Ou, and L. Mandel, *Phys. Rev. Lett.* **59**, 2044 (1987).
- [30] J. G. Rarity, P. R. Tapster, E. Jakeman, T. Larchuk, R. A. Campos, M. C. Teich, and B. E. A. Saleh, *Phys. Rev. Lett.* **65**, 1348 (1990).
- [31] J. Jacobson, G. Björk, I. Chuang, and Y. Yamamoto, *Phys. Rev. Lett.* **74**, 4835 (1995).
- [32] Y. H. Shih, A. V. Sergienko, M. H. Rubin, T. E. Kiess, and C. O. Alley, *Phys. Rev. A* **50**, 23 (1994).
- [33] M. H. Rubin, D. N. Klyshko, Y. H. Shih, and A. V. Sergienko, *Phys. Rev. A* **50**, 5122 (1994).
- [34] R. Landauer, *Phys. Lett. A* **217**, 188 (1996); C. H. Bennett, *Physica D* **86**, 268 (1995).
- [35] W. Holladay, *Phys. Lett. A* **183**, 280 (1993); T. F. Jordan, *Phys. Rev. A* **48**, 2449 (1993).